Vol. 28 Nos. 125/126 *Journal of the Radio Research Laboratories* *March/July 1981*
Printed in Tokyo, Japan *pp. 35–48*

COSMIC RADIO NOISE AT HIGH FREQUENCIES AS OBSERVED WITH ISS-b

By
Minoru KOTAKI, Isao KURIKI
Chuuka KATOH and Hidetoshi SUGIUCHI

(Received on December 25, 1980)

ABSTRACT

Using the fixed-frequency receivers on Ionosphere Sounding Satellite (ISS-b) the average galactic radio noises have been measured at the frequencies of 5, 10, and 25 MHz. Since the receiving antenna used for satellite observation has generally such poor directivity, it is difficult to distinguish the direction of combing radio waves. Since ISS-b has a circular orbit of about 1000 km altitude, the strength of the galactic noise from the centre and anti-centre can be distinguished by the reason that the galactic centre is occulted by the earth at a certain position on an orbit.

The average brightness temperatures of the galactic radio noise at the frequencies of 5, 10, and 25 MHz have the values of $(1.71 \pm 0.48) \cdot 10^6$ K, $(4.15 \pm 1.05) \cdot 10^5$ K, and $(3.47 \pm 1.07) \cdot 10^4$ K, respectively. The radiated power coming from the direction of the galactic centre is higher than that of the anti-centre by 2.2 ~ 3.5 dB at high frequency band.

1. Introduction

The Radio Noise Measurement (RAN) is one of four missions of the Ionosphere Sounding Satellite (ISS-b), and the RAN mission is designed to observe all sorts of radio noise at the satellite altitude at four fixed frequencies, 2.5, 5, 10, and 25 MHz. ISS-b was launched on February 16, 1978 into an almost circular orbit with an altitude of about 1000 km, an eccentricity of 0.016, a period of about 107 minutes and an inclination of about 70°. The satellite is spin stabilized about the axis of the drum at a nominal value of 13.65 revolutions per minute. The absolute intensities of cosmic radio noises have been obtained from about ten months data since the satellite was launched.

In order to determine the local radio emissivity which is related to the interstellar electron spectrum, it is necessary to utilize the radio spectra in the various directions, such as the galactic centre, anti-centre, the north polar region and the direction of minimum radio brightness at lower frequencies. At the frequencies above 10 MHz, cosmic noise levels are well established from ground-based observations.[1],[2]. On the other hand, at the frequency below about 10 MHz these measurements are difficult to carry out from the ground because of the reflection and absorption effects by the ionosphere, and therefore the measurements have been made from rockets and satellites[3]–[7]. However the receiving antenna used has poor directivity, the resolution of the measurements is very bad. Therefore, the discrimination of the direction of incoming radio waves is difficult in most cases.

Because ISS-b has the circular orbit of about 1000 km altitude, the strength of the galactic noise from centre and anti-centre can be distinguished by reason that the galactic centre is occulted by the earth at a certain position on an orbit.

2. Instrumentation

The ISS-b spacecraft is a cylindrical drum about 82 cm in height and about 92 cm in diameter. The radio noise receiving system employs two pairs of dipole antennas with tip to tip lengths of about 36.8 m and 11.4 m, respectively, and they are mounted on the plane of rotation spaced 90° apart from each other. The monopole antenna which is used for calibration of the receiving system is mounted on the top cover with an inclination angle of about 60° and with a length of 20 cm. Passing through the matching networks, the signals received by the antennas are fed into the receiving equipment. The equipment is composed of four narrow band receivers operating at frequencies of 2.5, 5, 10, and 25 MHz, respectively. Each receiver includes the straight type amplifier to avoid the cross modulation produced by nonlinearities of the usual heterodyne amplifier. To obtain the absolute values of radio noise intensities, the receiving systems including antennas were calibrated before being loaded onto the satellite. In order to obtain the total characteristics of the receiving systems, the dummy antenna circuit which has the same input impedance as the dipole antenna is connected to the receivers via the matching networks, and examined for the output values corresponding to input signals.[8]

In order to monitor the relative changes of the characteristics of the total receiving system, that is, to confirm the variation of the characteristics with the lapse time in short or long term, or the variation under the influence of spatial variation of the plasma density surrounding the antenna, the signal intensities are stabilized within two percent of the mean level and fed to the calibration-antenna. The calibration-antenna is coupled to the dipole

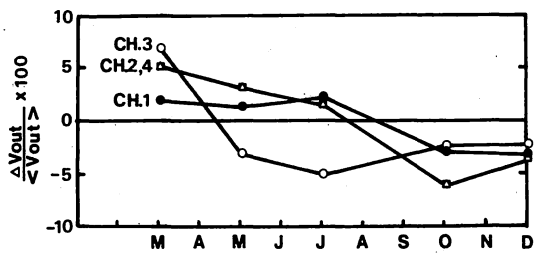

Fig. 1 Long-term variations of the receiving system.

antennas via space with the coupling loss of 61 ~ 71 dB in free space. Figure 1 shows the long-term variations of the output levels of the calibration signal received in each channel during the period from March to December of 1978, and the data used for the analysis of the cosmic radio noise were obtained in the same period. It is seen from the figure that the long-term variations of the receiving systems are negligible for all channels, because the degrees of variation lie within about 5 %. Furthermore, in order to see the long-term vari-

ation of characteristics of the receiver itself, the internal noise level in the receiver was monitored with the input terminal of receiver switched from antenna to 75Ω resistor. Figure 2 shows the variation of the internal noise of the receiver in every channel from March to December, 1978. As seen from the figure, the fluctuations of the internal noise level are so small that the characteristics of the receiver seem also to be fairly stable for the observation period.

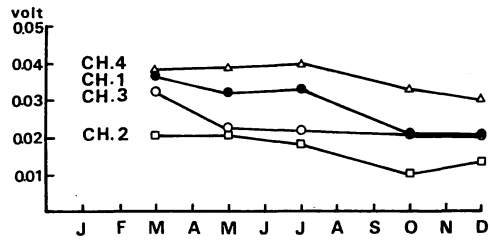

Fig. 2 Long-term variation of the receiver's internal noise levels during the period from March to December, 1978.

3. Observation

In addition to radio noise observation (RAN), the ISS-b has three other missions which provide the ambient plasma parameters in the topside ionosphere, such as the temperature, the electron density and the ion composition at the satellite height. These four observations are executed repeatedly in a period of 64 seconds and the RAN equipment operates during 24 seconds in every 64 seconds. External radio noise measurements are performed during the first 20 seconds, the total gains of the receiving system including the antennas are then calibrated during the next 2 seconds and lastly internal noise levels of the receivers are recorded during 2 seconds.

There exist some radio emissions which disturb the observation of the cosmic radio noise, *i.e.*, solar burst or interferences from transmitters on the ground. Because the RAN equipment is oeprating at fixed frequencies continuously, we can obtain information about the successive intensity variation of received radio noise. It is easy to identify the cosmic radio noise whose fluctuation is very small compared with the solar radio emission or interferences whose intensities show drastic changes with time and space. Figure 3 shows an example of the cosmic radio noise observed in one observational period (24 seconds) by ISS-b. The figure has frames which show the output levels of received radio noise of CH.1 (2.5 MHz), CH.2 (5 MHz), CH.3 (10 MHz), and CH.4 (25 MHz) from the top frame to the bottom, respectively. The abscissa indicates the time in seconds and the ordinate shows the analog output levels in the range of $0 \sim 2.5$ volts which nearly correspond to $-120 \sim -60$ dBm at the input terminal. As is evident from the figure, the intensity of cosmic radio noise has almost constant values for each channel. Since the plasma frequency at the satellite height (about 1000 km) changes in the range for $0.5 \sim 3$ MHz, the variation of the analog output level of CH.1 is fairly large, following the change of the medium in time and space.

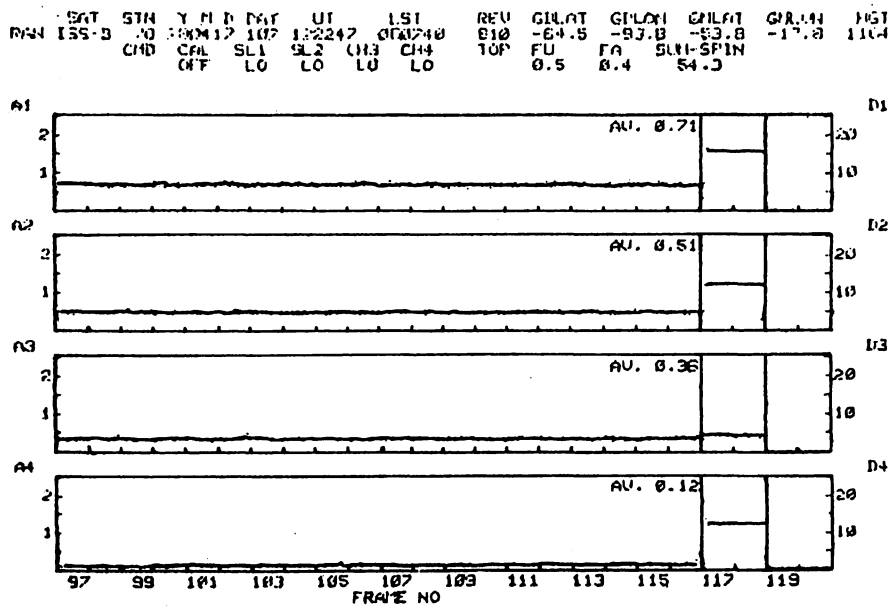

Fig. 3 An example of cosmic radio noise observed by ISS-b during one observational period (20 seconds).

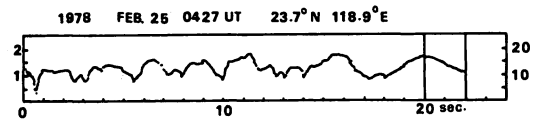

Fig. 4 The variation of the calibration wave received in CH.1 (2.5 MHz).

As in Figure 4 which shows the variation of the calibration signal radiated from short monopole antenna received in CH.1, the incoming radio waves with the frequency of 2.5 MHz may be largely absorbed by the plasma medium surrounding the satellite.

The ISS-b is spin stabilized with a nominal value of 13.65 rpm and the axis oriented in the direction of about 60° in declination and about 7 hr in right-ascension in the equatorial coordinate system with slow precession as in Figure 5. The direction of the spin axis and its opposite direction point to the area bounded by a thick line in Figure 6 which shows the distribution of the galactic noise intensity measured at frequency of 100 MHz[9]. As the dipole antennas are mounted on the plane perpendicular to the spin axis, the effective aperture of the antennas points nearly to the direction of the galactic centre (−30° in declination, 18 hr in right-ascension) and anticentre (60° in declination, 6 hr in right-ascension). Depending on the location of the satellite on the circular orbit, the radio noise coming from the

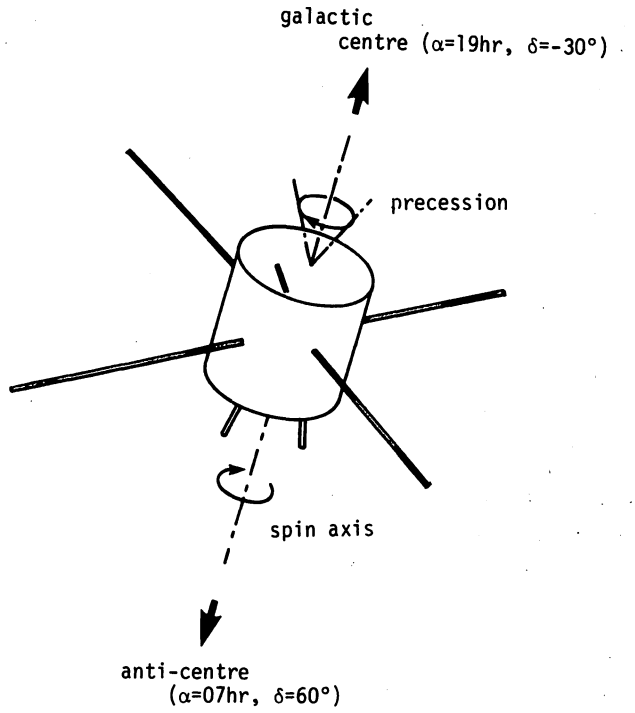

Fig. 5 A geometrical schema of the ISS-b.

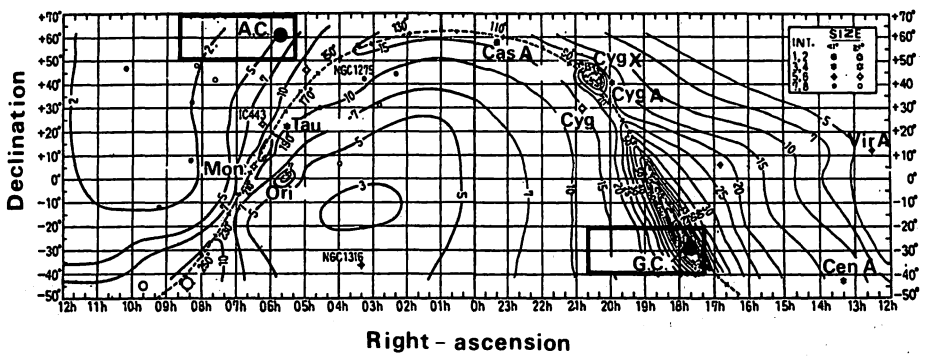

Fig. 6 The direction of the spin axis points to the squared area plotted on the brightness observed at 100 MHz. Black spots denoted by "GC" or "AC" in the figure are the direction of the galactic centre and the anti-centre, respectively.

galactic centre cannot be received by the satellite because of the occulation of the coming wave by the earth (refer to Appendix). The earth is surrounded by the plasma-sphere; what is more, the area in which the satellite cannot observe the radio wave coming from the galac-

tic centre changes with complexity depending on the frequency of the radio wave and the electron density of the medium. Generally, the area of the galactic centre shielded by the earth decreases with increasing radio frequency (refer to the Appendix).

4. Observation results

4.1 Average intensity

The data of about 80 orbits used for the statistical analysis were obtained from March to December 1978. To obtain the radio noise intensity it is necessary to convert the intensity observed in the plasma medium into the observable value in free space. The plasma frequency of the medium (f_{ns}) at the satellite height depends on the location of the satellite, the local time and the solar activity. The noise power P_s (W) measured in a medium of refractive index n is related to the noise power P_o (W) in free space by $P_o = P_s/n^2$, and $n^2 = 1 - (f_{ns}/f_{obs})^2$ where f_{obs} is the observing frequency.(7) The plasma frequency (f_{ns}) at the satellite height ranges from 0.5 ~ 3 MHz and usually it is about 1 MHz in the nighttime and 2 ~ 2.5 MHz in the daytime.(10) It is necessary to make a considerable correction, by the reason mentioned above, for the measured value at CH.1 (2.5 MHz) observed in the daytime, and therefore, we do not include the value observed at CH.1 in the present statistical result. On the other hand, as for the observation frequency above 5 MHz, it seems to be quite all right to identify the noise power P_s measured in a medium as P_o observable in free space. If the plasma frequency (f_{ns}) takes the value of 2.5 MHz and the observing frequency is 5 MHz, for example, P_o/P_s becomes 0.75, then the error due to identifying P_s as P_o becomes about 1.2 dB (= $10 \cdot \log P_o/P_s$); therefore, it is not so large and probably comparable with the experimental uncertainties. Considering the facts described above, the cosmic radio noise intensities are derived as follows.

The available noise power W_a (W) for the dipole antenna is related to the power flux density P_n (W/m^2 · Hz) for one component of polarization of the incoming radio wave as follows:

$$W_a = (\lambda^2/4\pi) \cdot P_n \cdot g \cdot b \qquad (1)$$

where λ is the wavelength (m), b is the effective receiver bandwidth (Hz) and g is the gain factor of the dipole antenna over the isotropic antenna. As the cosmic radio noise should be considered to be nearly randomly polarized, the practical flux density of the coming radio wave P_s (W/m^2·Hz) takes the duplicated value of P_n, *i.e.*, $P_s = 2 \cdot P_n$. Assuming that the dipole antennas have effective apertures of 4·π steradians, the brightness I (W/m^2·Hz·sterad.) can also be derived from

$$I = P_s/4\pi = 2 \cdot k \cdot T_a/\lambda^2 \qquad (2)$$

where k is Boltzmann's constant (1.38×10^{-23} Joules/K) and T_a (K) is the effective antenna temperature. The values obtained from ISS-b observation are considered to be the average cosmic noise level because they include the radio waves coming from all directions. In this way, the cosmic radio noise levels are obtained from March to December 1978, corresponding to the data for about 140 hours. The cosmic radio noise temperatures obtained are summarized as $(1.71 \pm 0.48) \times 10^6$ K, $(4.15 \pm 1.05) \times 10^5$ K, and $(3.47 \pm 1.07) \times 10^4$ K at 5,

10, and 25 MHz, respectively, and the results are listed in Table 1.

Table 1 Cosmic radio noise intensity at CH.2 (5 MHz), CH.3 (10 MHz), and CH.4 (25 MHz).

channel	2	3	4
Wa (dBW)	−136.74 + 1.26	−143.15 + 1.12	−152.17 + 1.38
I (W/M^2·Hz·sterad.)	(1.31 ± 0.37) 10^{-20}	(1.27 ± 0.32) 10^{-20}	(6.66 ± 2.05) 10^{-21}
Ta (K)	(1.71 ± 0.48) 10^6	(4.15 ± 1.05) 10^5	(3.47 ± 1.07) 10^4

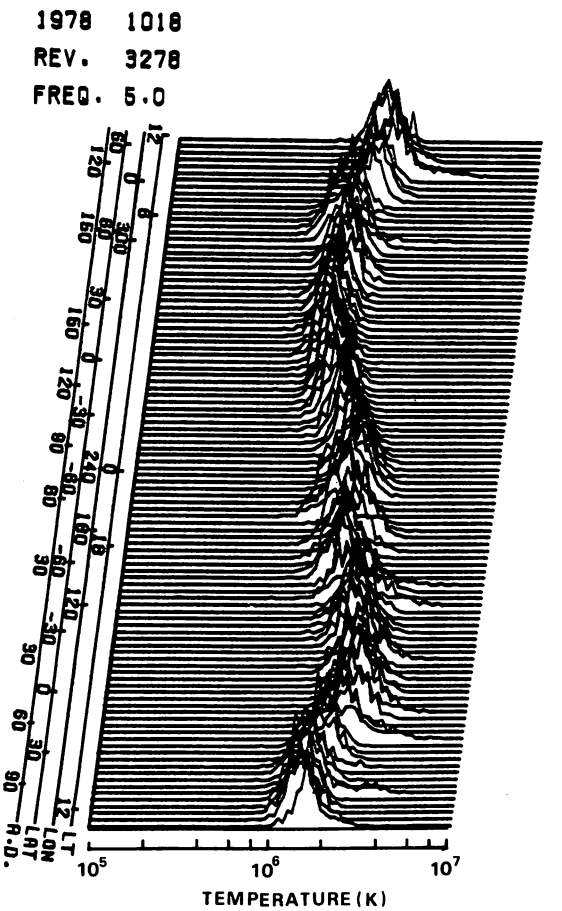

Fig. 7 The variation of cosmic radio noise temperature observed at 5 MHz along an orbit around the earth.

4.2 Noise powers from galactic centre and anti-centre

By utilizing the effect of the occultation by the earth, we can distinguish the galactic radiation in the direction of the centre and anti-centre. Figure 7 shows the variation of radio noise intensity at 5 MHz observed along an orbit around the earth. During the satellite circulating around the earth, about 100 times of the observations are performed, and 560 measured values for each channel are obtained in one observation period of 20 seconds.

The abscissa (X axis) in figure 7 indicates the radio noise intensity scaled in termperature, and the ordinate (Y axis) shows the location of the satellite. Each undulating line parallel to the abscissa corresponds to the observed noise temperature given by the abscissa during one observation period (20 seconds). The amplitude (Z axis) of the undulating line indicates the occurrence numbers out of 560 values, and therefore, the position of maximum amplitude on the abscissa corresponds to the average noise level over the observation period. The ordinate indicates the satellite location such as the longitude, the latitude, the local time and the angular distance (A.D.) which is the angle between the line connecting the centre of the earth and the galactic centre and the line connecting the centre of the earth and the satellite. Figure 7 shows that the noise temperature rises as the angular distance (A.D.) decreases, and it takes the maximum value of about 2×10^6 K at the angular distance less than 30°, that is, when the satellite is located in the direction of the galactic centre. On the other hand, the noise temperature decreases as the angular distance increases, and the temperature takes the minimum value of about 9×10^5 K at the angle greater than 150°.

As the main lobe of the antenna faces nearly in the direction of the galactic centre and anti-centre, it becomes possible to distinguish between the radio noise coming from the direction of galactic centre and that from the anti-centre by the occultation effects of the earth. To minimize the effect of ambient plasma around the satellite, in estimating the galactic noise intensities for CH.1 (2.5 MHz) and CH.2 (5 MHz), we make use of the data observed only in the daytime. Since the plasma frequency at the satellite height may be about 1 MHz in the nighttime, the errors due to identifying the observing intensity with the radio noise intensity in free space may become about 0.76 dB at CH.1 and about 0.18 dB at CH.2. Therefore, these errors seem to be negligible.

Receiving powers W_a (W) of the radio noise coming from the galactic centre at the frequencies of 2.5, 5, 10, and 25 MHz are −129.9, −135.1, −142.3, and −149.7 dBW, respectively. Using the equation (1) and (2), these values are transformed to the brightness of the incoming radio noise as listed in Table 2.

Table 2 Radio brightness in the direction of the galactic centre and anti-centre ($W/m^2 \cdot Hz \cdot sterad.$).

channel	1	2	3	4
Galactic centre	1.73×10^{-20}	1.90×10^{-20}	1.54×10^{-20}	1.15×10^{-20}
Anti-centre	7.68×10^{-21}	9.21×10^{-21}	9.20×10^{-21}	5.37×10^{-21}
G.C./A.C.	2.25	2.06	1.67	2.14

5. Concluding Remarks

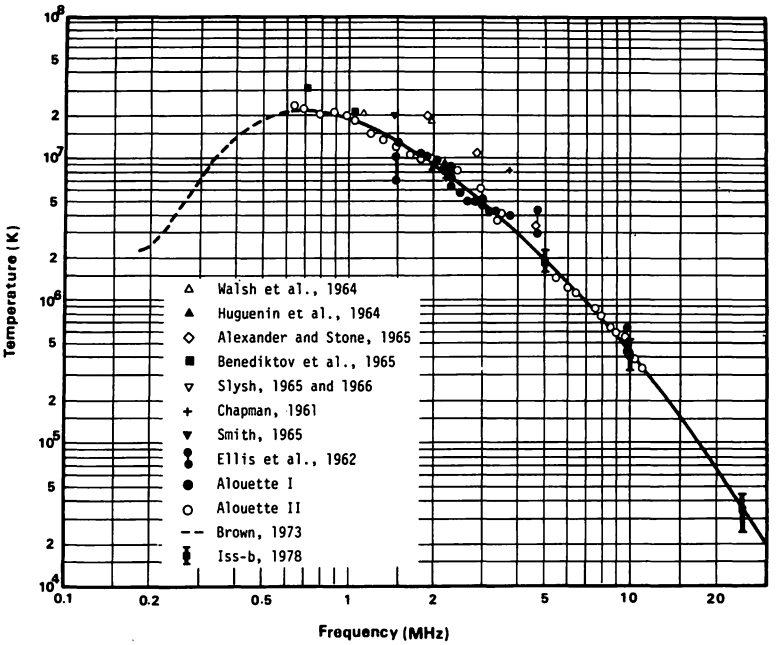

Fig. 8 Effective cosmic noise temperatures measured in rockets and satellites.

Figure 8 shows that the observational results obtained by ISS-b in the way described above compare favorably with previous measurements making use of rockets or satellites.[11] In the figure, the tips of the rod which show the measurement results of ISS-b indicate the standard deviation from the mean value. The abscissa and ordinate show the frequency and the effective noise temperature.

The radio brightness in the direction of the galactic centre observed by ISS-b at frequencies of 2.5, 5, 10, and 25 MHz is shown in Figure 9 together with previous measurements.[12] The radio noise intensity in the direction of the galactic centre is 1.67 ~ 2.25 times higher than that of the anticentre as is shown in Figure 9 and Table 2. Even though the radio noise intensity is a value in a certain direction, however, it should be mentioned that the observed values include the radio noise coming from quite a wide source region because of the broad antenna pattern. The occultated source region of incoming radio wave expands over roughly $\pi \sim 3\pi$ steradians. (see the Appendix)

Acknowledgement

In preparing for this paper, the authors are deeply indebted to all members concerned in the ISS-project, especially to the members of ISS Research and Operation Committee.

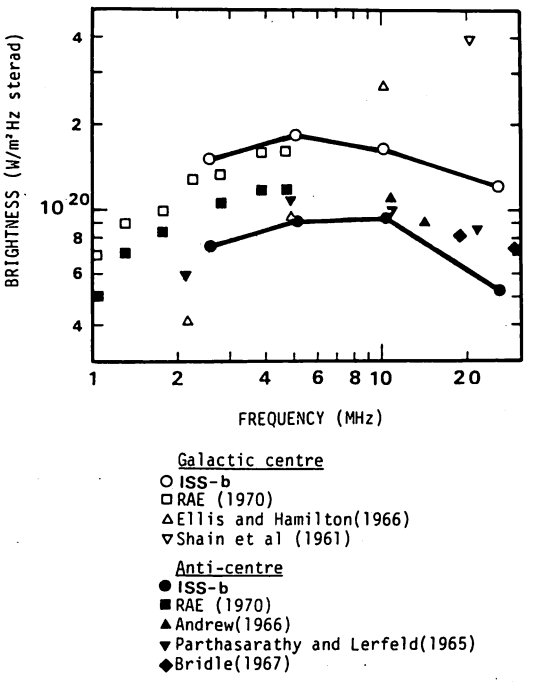

Fig. 9 Radio brightness spectra in the direction of the galactic centre and anti-centre.

Thanks are also due to the tracking and telemetry staffs of Kashima-branch and to the data reduction and analysis groups of Radio Research Division. Sincere thanks are also due to participants of NASDA for their collaboration.

References

(1) Andrew, B.H.; "The spectrum of low radio frequency background radiation.", Mon. Not. R. Astr. Soc., **132**, 79, 1966.

(2) Getmantsev, G.G., Karavanov, V.S., Korobkov, Y.S., and Tarasov, A.F.; "Frequency spectrum of the distributed cosmic radio emission in the range from 6.3 to 40 MHz." Astronomical J., **45**, 936, 1968.

(3) Alexander, J.K., and Stone, R.G.; "Rocket measurements of cosmic noise intensities below 5 Mc/s", Astrophys. J., **142**, 1327, 1965.

(4) Smith, F.G.; "Cosmic radio noise as measured in the satellite Ariel II; Part II, Analysis of the observed sky brightness.", Mon. Not. R. Astr. Soc., **131**, 145, 1965.

(5) Hartz, T.R.; "Observations of the galactic radio emission between 1.5 and 10 Mc/s from the Alouette Satellite.", Ann. Astrophys., **27**, 823, 1964.

(6) Alexander, J.K., Brown, L.W., Clark, T.A., Stone, R.G., and Webber, R.R.; "The spectrum of the cosmic radio noise background between 0.4 and 6.5 MHz.", Astrophys. J., **157**, 1163, 1969.

(7) Hakura, Y., Nishizaki, R., and Tao, K.; "Analysis of observational data obtained by Alouette II; 4. Galactic noise spectrum and solar radio bursts in hectodecametric wave region.", J. Radio Res. Labs., **16**, 215, 1969.
(8) Katoh, C., Kuriki, I., Kotaki, M., and Sugiuchi, H. Characteristics of radio noise observation equipments., to be published in ISS-b special issue., 1981.
(9) RIKA-NENPYOU, Edited by Astronomical Observatory, MARUZEN, 1980.
(10) Miyazaki, S. *et al.*, to be published in ISS-b special issue.
(11) CCIR. Report 342-2, Radio noise within and above the ionosphere, 1974.
(12) Webber, W.R.; "On the relationship between recent measurements of galaxy, and the solar modulation of cosmic rays.", Aust. J. Phys., **21**, 845, 1968.
(13) Jones, R.M., and Stephenson, J.J. A versatile three dimensional ray tracing computer program for radio waves in the ionosphere, OT-Report, 75–76, Oct. 1975.

Appendix Occultation effects

When we observe radio waves coming from distant sources, such as solar radio waves, cosmic radio waves, Jovian radio waves, by satellite, according to the location of the satellite soaring near the earth, there exist some unobserved regions as a matter of cause. The extent of the unobserved region depends on the radio frequency and the electron density distribution of the ionosphere. Considering the case of ISS-b, the extent of such region is studied by computing ray trajectories in numerically assumed electron density distributions.

A-1 Calculation method

As in Figure A-1, the model ionosphere used in the calculation is assumed as follows. The critical frequency of the F layer (f_c) is 10 MHz and its maximum height h_mF is about 300 km and the profile above h_mF consists of a Chapman-layer with variable scale height; that is, the plasma frequency (f_n) at the height of h km ($h > h_mF$) is given as follows: follows:

$$f_n^2 = fc^2 \cdot \tau^{1/2} \cdot \exp\left\{(1-\tau)/2\right\} \quad \text{(A-1)}$$

where $\tau = (h_mF/h)^{\chi}$, $\chi = 8$.
We employed the magnetic field of earth's centered dipole model with the gyrofrequency at the equator on the ground of 0.8 MHz and with the north magnetic pole located at 78.5° N, 291° E in geographic coordinates.

Assuming that a radio source is located on the equatorial plane at a great distance from the earth, the plane wave is considered to come towards the earth parallel to the equatorial plane. Therefore, the calculation of the ray trace is started from 3000 km altitude as in Figure A-4. Namely, the assumption described above seems to be identical to the fact that the refractive index of the space at height above 3000 km is considered to be unity. According to the electron density distribution given in equation (3), the plasma frequency at 3000 km height becomes about 130 kHz. On the other hand, the ray tracing is performed in the frequency range above 1.3 MHz, and therefore, the assumption seems to be reasonable. the equations used for ray tracing were Hamilton's equations in four dimensions given by R.M. Jones and J.J. Stephenson, and the integration procedure used was a combination of the Adams-Moulton and Runge-Kutta method.(7)

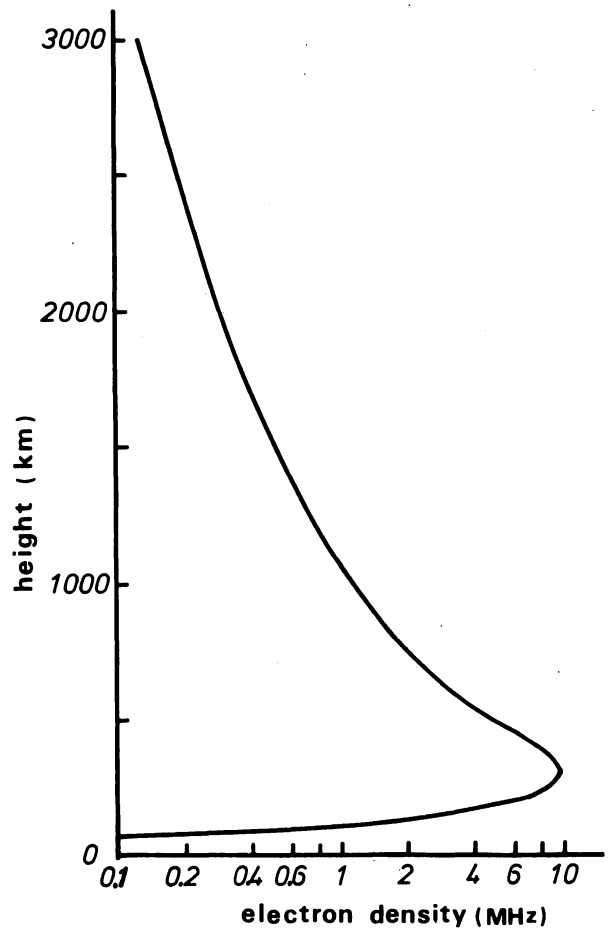

Fig. A-1 Electron density height profiles used for the ray tracing.

A-2 Results

The angle between the line connecting the earth's centre and the radio source and the line connecting the earth's centre and the boundary within which the coming radio wave can be observed is taken as a_{max} (refer to the figure A-4). And the angle between the line connecting the earth's centre and the satellite and the line connecting the earth's centre and the radio source is taken as a. The incoming radio wave can be received by the satellite if the angle a is less than the angle a_{max}.

When the electron density distribution is assumed to depend only on the altitude, disregarding the longitude or the latitude, the variations of the value, a_{max}, with the frequency of the coming radio wave in the meridian plane or the equatorical plane are shown in Figure A-2 as flat-layer. The ordinate of the figure shows the a_{max} in degrees and the abscissa indicates the ratio of the electron density at the height of 1000 km (f_{ns}) and the

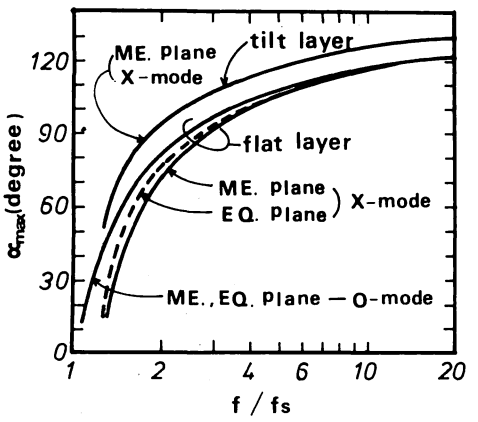

Fig. A-2 **The change of observable region with radio frequency.**

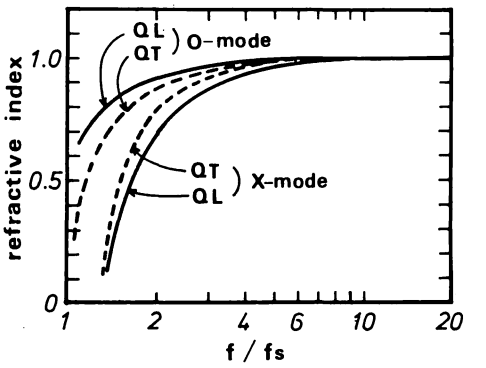

Fig. A-3 **The change of the refraction index at the satellite height with radio frequency.**

radio frequency (f). Decreasing the radio frequency, α_{max} takes different values for the ordinary (o-mode) or the extra-ordinary wave (x-mode) in the meridian or the equatorial plane, as may be seen from Figure A-2. The difference of the angle α_{max} for each mode may arise from the existence of the geo-magnetic field which causes the variation of the refractive index with the ray direction, as shown in figure A-3. Since α_{max} increases with increasing the refractive index, the coming radio wave with larger refractive index may be able to penetrate deeper into the ionosphere. The region where the incoming radio wave in x-mode of 15 MHz can be received in meridian plane is indicated by half shadow in Figure A-4, and the value of α_{max} is 119.1° in this case.

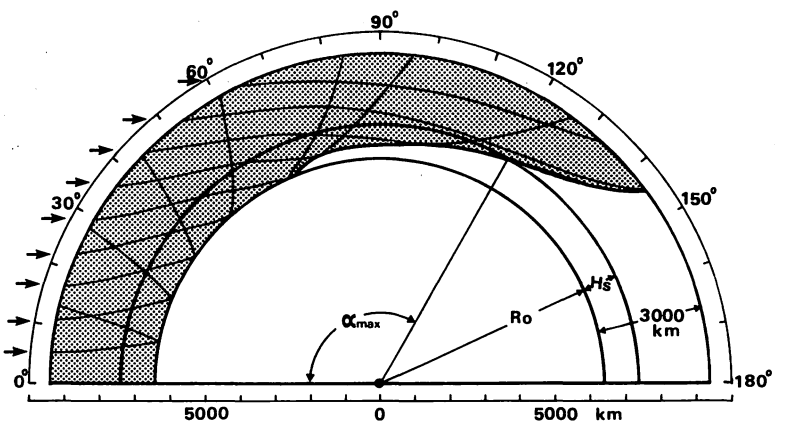

Fig. A-4 **An example of the observable region of coming radio wave at 15 MHz (shaded part). f_c = 10 MHz.**

Assuming the critical frequency of the ionosphere (f_c) decreases as the latitude (θ) increases, we estimate the value of α_{max}. f_c as follows:

$$f_c(\theta) = f_{ceq}^2 (1 - 0.75 \sin\theta) \quad \cdots\cdots\cdots\cdots\cdots\cdots\cdots\cdots \quad (A\text{-}2)$$

where f_{ceq} is the critical frequency at the equator ($\theta = 0°$).
Therefore, the critical frequency at the pole ($\theta = 90°$) takes a half value of the equatorical one. The estimated values of α_{max} for the ionosphere described above are indicated in Figure A-2 as tilt-layer. It is seen that the angle, α_{max}, of the tilted-layer takes quite different values from that of the flat-layer. When the wave frequency is large enough, $f/f_{ns} = 20$ for example, α_{max} is about 130°, whereas the fact is that α_{max} with no existence of the ionosphere should take the value of about 120° as is given from a simple geometry.

In generally, the receivable region of the incoming wave becomes narrow due to the existence of the ionosphere. However, in the case of tilted ionosphere, the region becomes wider than that for the light according to the wave frequency as described above.

As the ionosphere changes complicatedly with time and space in practice, it is difficult to estimate the extent of the receiving region (or the unreceiving region because of the occultation effect). Broadly speaking, the extent of the occulted radio source region (ω steradian) can be expressed as follows:

$$\begin{aligned} \omega &= 2\pi \left\{ 1 - \cos(180° - \alpha_{max}) \right\} \\ &= 2\pi (1 + \cos\alpha_{max}) \quad \cdots\cdots\cdots\cdots\cdots\cdots\cdots\cdots\cdots\cdots \quad (A\text{-}3) \end{aligned}$$

Therefore, the extent of the occulted source region changes with α_{max}, and the value of α_{max} depends on the electron density distribution of the ionosphere. Now we estimate the typical values of ω for the daytime and the nighttime. If the plasma frequency (f_{ns}) at the altitude of 1000 km is assumed to be 1 MHz in the nighttime, the extent of the occulted region (ω) can be estimated from equation (A-3). Using the values of α_{max} given in figure A-2, the extent of the occulted regions becomes 2π steradian for CH.1 (2.5 MHz), 1.4π steradian for CH.2 (5 MHz), 1.1π steradian for CH.3 (10 MHz), and 0.9π steradian for CH.4 (25 MHz). In the daytime, on the other hand, the typical plasma frequency at the altitude of 1000 km is assumed to be 2 MHz; then the values of ω at the radio frequency of 2.5, 5, 10, and 25 MHz are 3.4π, 2π, 1.4π and π steradians respectively. It is seen that the source region occulted by the earth decreases as the radio frequency increases.